Full Paper Transactions, SMiRT 28
Toronto, Canada, August 10-15, 2025

BUCKLING ANALYSIS OF LFR-AS-30 FUEL ASSEMBLIES UNDER SEISMIC LOADING CONSIDERING FLUID STRUCTURE INTERACTION EFFECTS

Pietro Gulinelli[1], Alessandra Perrone[2], Stefano Cristofanelli[3] Andrea Mazza, Peter James Cochran, Andrea Barbensi

[1] Mechanical Analyst, PhD, Newcleo spa, Turin, Italy (pietro.gulinelli@newcleo.com)
[2] Mechanical Analyst, Newcleo spa, Turin, Italy (alessandra.perrone@newcleo.com)
[3] Structural Analysis Head of Unit, Newcleo spa, Turin, Italy (stefano.cristofanelli@newcleo.com)

ABSTRACT

An application of the acoustic FEM to the seismic analysis of Newcleo's LFR-AS-30 is presented in the current work focusing on the buckling of core structures. A FSI model of the reactor block is implemented in Ansys and used to compute seismic loads due to fluid hydrodynamic pressures and structure acceleration. These are then transferred to a refined model of the fuel assembly, on which buckling calculations are performed including static load contributions. Two modelling techniques of the reactor plenum are proposed to investigate the influence of sloshing on the seismic behaviour, enabling to identify the most critical buckling collapse modes of the fuel assemblies.

1. INTRODUCTION

Fluid-structure interaction (FSI) represents a critical aspect in the fulfilment of the safety requirements of a pool-type Lead-cooled Fast Reactor (LFR). Indeed, the high density of the lead and its motion during a seismic event may induce significant overpressures on the main vessel and on the internal immersed components. The understanding of these phenomena is even more crucial for core structures, which are not only subjected to oscillations affecting reactivity, but also to a high risk of structural failure. The seismic analysis of the Newcleo LFR, hereafter denoted as LFR-AS-30, is presented in this study, focusing on the effect of FSI on the buckling of Fuel Assemblies (FAs), which represent the elementary core units. The LFR-AS-30 is an irradiation reactor in fast flux, demonstrator of the LFR technology. The global features of the reactor are reported in Table 1.

Table 1. LFR-AS-30 global design features.

Power	30 MW_{el}
Core coolant	Pure lead
Fuel	MOX

In the last decades, the increasing awareness of the potential hazard to the nuclear plants from earthquakes was accompanied by the development of several analytical and numerical methods for modelling FSIs. The analytical method consolidated in national and nuclear engineering codes (cf. Eurocode 8, ASCE, NZSEE) provide estimations about sloshing and impulsive frequencies and masses, and about hydrodynamic pressures due to seismic acceleration, for simple geometries and boundary conditions (typically base-supported fluid-filled cylindrical tanks with rigid walls). Further developed analytical solutions for suspended flexible vessels and immersed components are present in literature, as Yu and Whittaker (2020-2021), Kangda et al. (2016), but still limited to simple geometries (such as concentric cylinders). Numerical methods as FEM (Finite Element Method), CFD (Computational Fluid Dynamics) and ALE (Arbitrary Lagrangian Eulerian) enable a more general modelling approach. The acoustic FEM is the method currently used in Newcleo, and consists of meshing the fluid volume with suitable pressure-based acoustic fluid elements, allowing to directly model sloshing effects and FSI at immersed internals, cf. Sigrist (2007). The seismic response in terms of fluid hydrodynamic pressures and structural displacements is obtained via a modal analysis and a subsequent spectrum analysis. Application examples of this method on LFR and PWR (Pressurised Water Reactors) are reported by Platti (2015) and Je et al. (2017).

In the current work, a simplified FSI model of the LFR-AS-30 including the core is implemented in Ansys APDL (Ansys Parametric Design Language) by means of acoustic fluid elements. The computed seismic response is then transferred to a more refined sub-model of the fuel assembly to calculate buckling modes. The document is organized as follows. The calculation methodology is presented in section 2. Results are reported in section 3. Conclusions and related future works are finally outlined in section 4.

2. METHODOLOGY

The calculation flowchart is shown in Figure 1, highlighting the analysis steps and the associated FE models. The seismic analysis (step 1) is performed with the FSI model of the reactor block, characterised by an average element size of 30 mm. The main features of the FSI model are summarised in Table 2. The reactor core is divided into 37 fuel assemblies, each one composed by a wrapper (lower hexagonal box containing the fuel active zone), a bulkhead (upper massive part), and a shaft connecting wrapper to bulkhead. The mass of the active zone and of the lead contained in the wrapper is spread on the wrapper walls, which are modelled with equivalent shell elements. Assembly-assembly and assembly-inner vessel contact interactions are modelled via displacement constraint equations, whose location is indicated by “CEX/Y/Z” in Figure 1. The fluid domain is meshed with acoustic fluid elements (fluid220). FSI at core-lead surfaces is handled by means of contact elements, while mesh topologies of fluid and all the other structures are shared. The roof external edge is fixed.

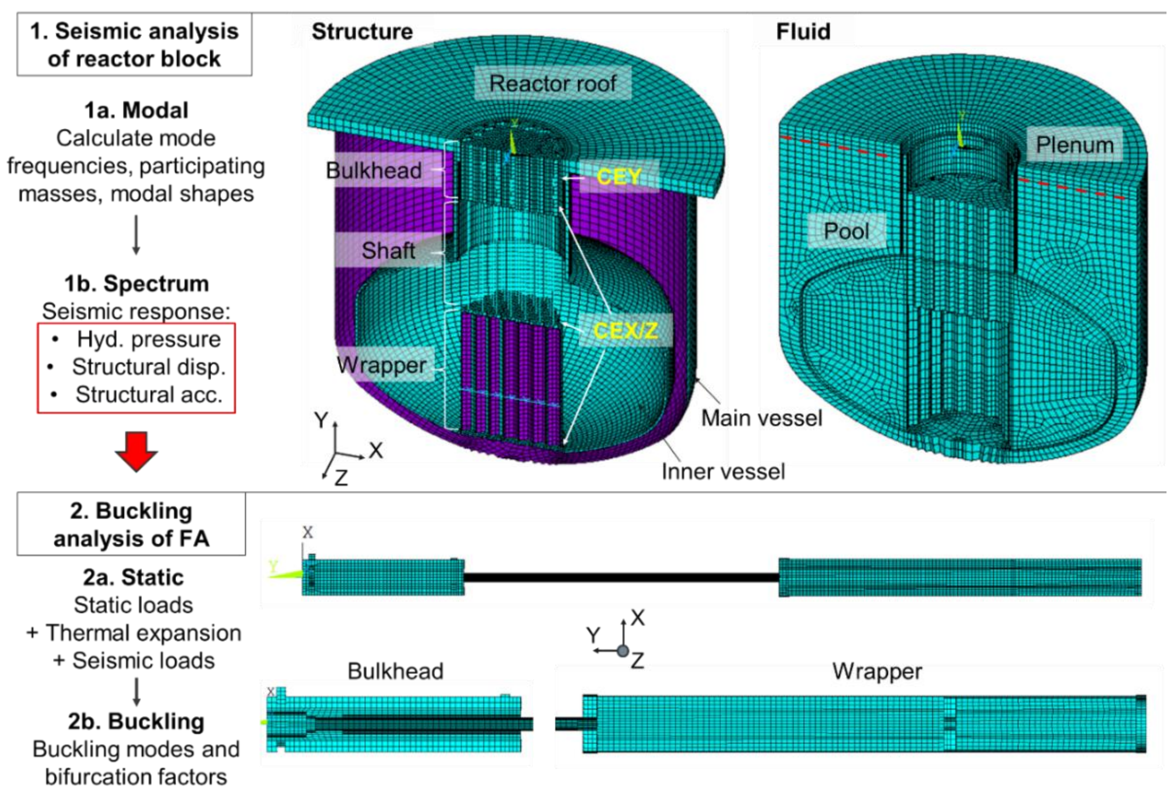

Figure 1. Calculation flowchart.

The refined model of the FA (step 2) is entirely meshed with solid elements with an average size of 20 mm. All elements are quadratic (with mid-nodes) for both models. Material properties of structures and fluid at 420°C are considered[1], and they are provided in Table 3 according to RCC-MRx, for stainless steel 316, and Panico, Tomatis (2023), for lead.

Table 2. FSI model main features.

Total mass	890 t
Total height	5 m
Vessel diameter	5 m
Plenum height	200 mm

Table 3. Material properties (420°C).

Material	E [GPa]	ν	ρ [kg/m^3]
Stainless Steel 316	172	0.3	8000
Lead	-	-	10554

Response spectra (acceleration vs frequency) used in the spectrum step (1b, cf. Figure 1) were calculated within Newcleo based on the installation site and on the reactor building, and are reported in Figure 2a. Acceleration peaks are located in the range 4-20 Hz, and reach 1.8-1.9 G for horizontal directions (X and Z) and 1.3 G for the vertical direction (Y). According to Regulatory Guide 1.92, the seismic response transferred to the FA model is obtained by the Newmark combinations expressed in Eq. (1), where “R” is the response in terms of fluid hydrodynamic pressures, structural displacements and structural accelerations, while the subscripts “144”, “414”, “441” indicate the main excitation direction[2].

The main limit of this kind of analysis is the incapability of modelling non-linear FSI phenomena as the impact of sloshing waves on the vessel roof. The two options of linear plenum modelling shown Figure 2b are thus proposed:

A. Lead plenum: the plenum is meshed via acoustic fluid elements with lead density (cf. Table 3). FSI between lead plenum and surrounding structures. Sloshing is not allowed.
B. Empty plenum, sloshing at lead free level is allowed.

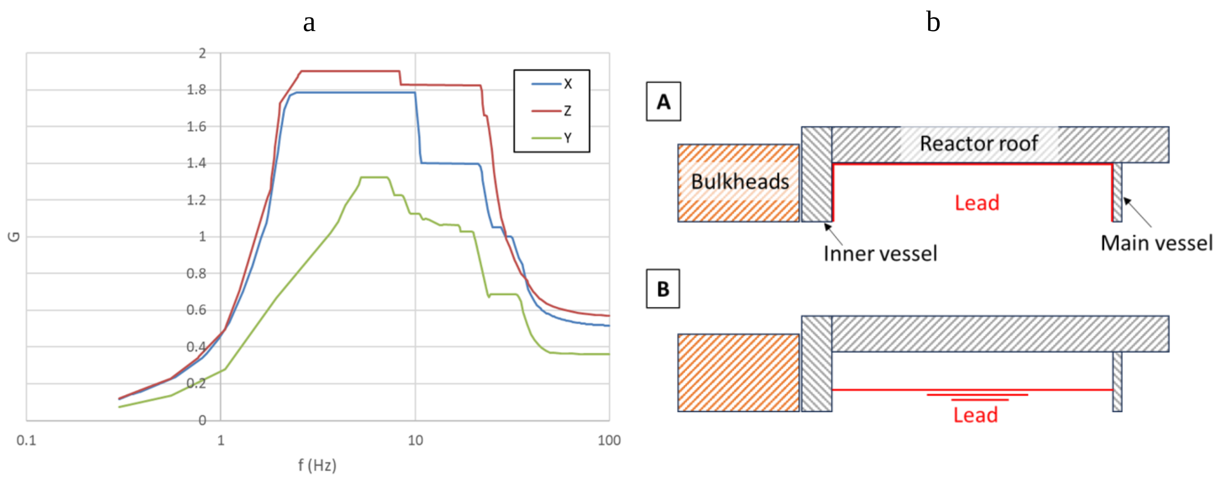

Figure 2. (a) Response spectra; (b) Studied options of plenum-pool interfaces.

$$\begin{aligned} R_{144} &= \{R_X + 0.4R_Y + 0.4R_Z\} \\ R_{414} &= \{0.4R_X + R_Y + 0.4R_Z\} \\ R_{441} &= \{0.4R_X + 0.4R_Y + R_Z\} \end{aligned} \quad (1)$$

[1] Since the process must work at temperatures higher than 330°C (lead freezing), a working temperature of 420°C was selected for the scope of the current analysis.
[2] The directional responses R_X, R_Y and R_Z are computed by algebraic sum of the mode responses with the highest participating masses (see results).

3. RESULTS

Results hereafter presented are organized as follows. Results of reactor block seismic analysis are reported in section 3.1. Results of fuel assembly buckling analysis are then presented in section 3.2. The presented outcomes must not be intended as the final results of the current configuration of the LFR-AS-30. The final design may be affected by other loads not considered at this stage

3.1. Seismic analysis of the reactor block

The mode frequencies (eigenvalues) associated to the highest participating masses (highest m/m_{tot}, with m_{tot} = 1000 t, cf. Table 2) resulting from modal analysis are reported in Table 4 for options A and B (cf. Figure 2b). The corresponding displacement and pressure shapes (eigenvectors) associated to horizontal (X/Z) and vertical (Y) are shown in Table 5 and Table 6, respectively (modes with similar eigenvectors are designated with the same mode id.). The rows denoted with "Tot." indicate the total percentage of mass extracted in the modal analysis, in the range 0-100 Hz.

Concerning horizontal directions, modes 4 and 5 (8-12 Hz) are those characterised by the highest participating masses and correspond to in-phase motions of core, inner vessel, and main vessel of 1st and 2nd order[3], respectively. Mode 3 (1.67 Hz) corresponds to the out-of-phase motion of the core-inner vessel system with respect to the main vessel, and it is associated to a much lower m/m_{tot}. Modes 1 and 2 correspond to sloshing at low frequency (0-1 Hz, cf. Table 5) and are thus obtained only for option B. It can be remarked that options A and B have similar total m/m_{tot}, despite the absence of sloshing in option A. This is an important outcome, since including sloshing in the calculation significantly increases the computation time.

Concerning vertical directions, A and B show a similar behaviour. Notably, mode 1 is associated to core compaction/expansion, while mode 2 corresponds to a vertical displacement of central fuel assemblies.

Table 4. Results of modal analysis: mode frequencies (eigenvalues) and associated m-to-m_{tot} ratios.

		A		B	
Direction	Mode id.	f [Hz]	m/m_{tot} [%]	f [Hz]	m/m_{tot} [%]
X/Z	1	-	-	0.36	18.15
	2	-	-	0.72	2.72
	3	-	-	1.67	3.03
	4	8.21	77.40	8.84	35.26
	5	10.0	12.20	11.19	30.76
	Tot.	-	98	-	96
Y	1	9.43	89.54	9.40	90.16
	2	15.40	3.26	15.32	3.26
	Tot.	-	99	-	99

[3] The order identifies the number of sinusoids determining the structure deformed shape.

Table 5. Modal analysis, X/Z directions: displacement and pressure modal shapes (eigenvectors).

Mode id.	Displacement (UX) 0 Umax	Pressure (PRES) Pmin Pmax
1	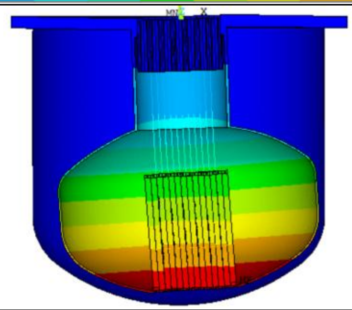	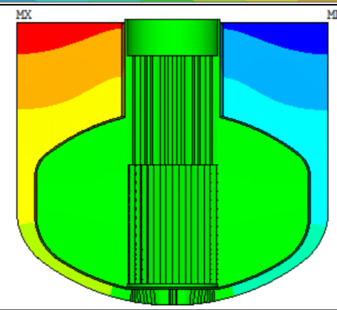
2	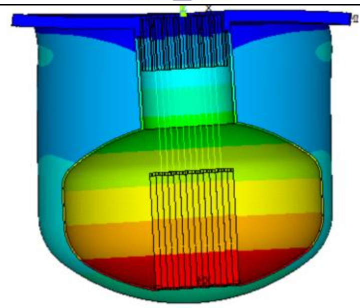	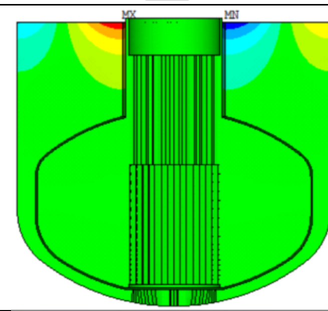
3	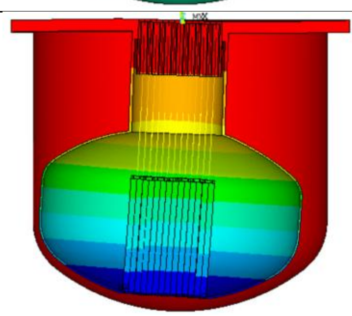	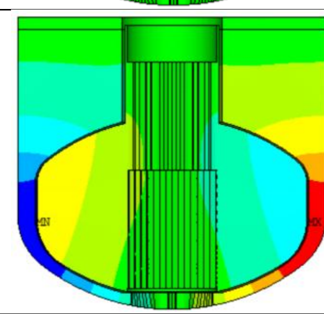
4	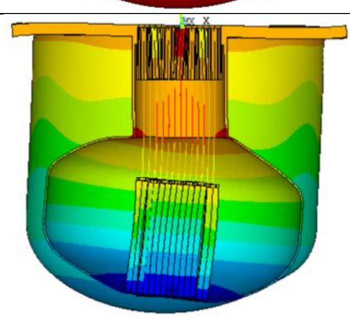	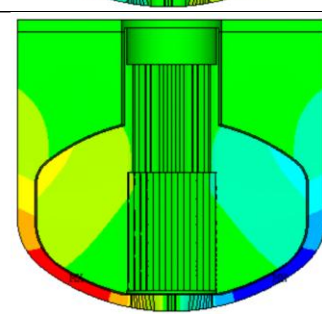
5	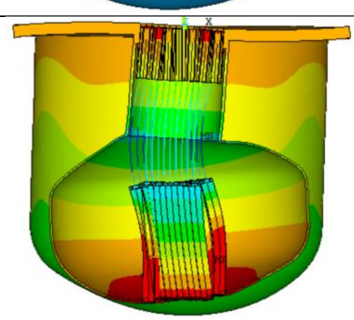	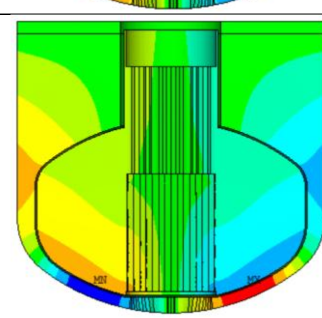

Table 6. Modal analysis, Y direction: displacement and pressure modal shapes (eigenvectors).

Mode id.	Displacement (UY) 	Pressure (PRES) 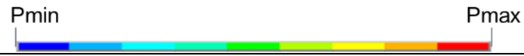
1	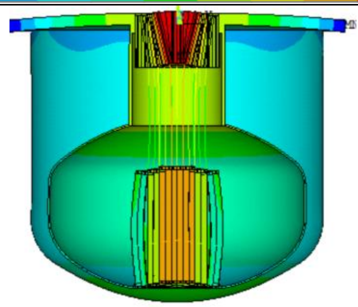	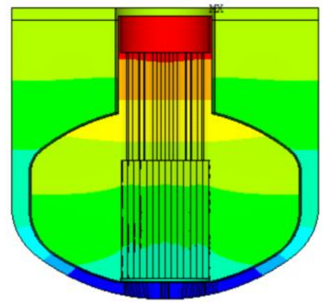
2	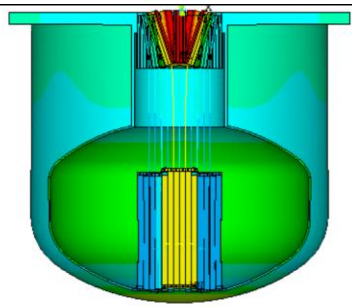	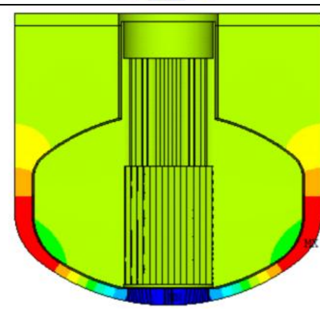

Spectrum responses R_{144} and R_{414} obtained via Eq. (1) are shown in Table 7 for option A, and in Table 8 for option B. Displacement and pressure distributions associated to R_{441} are similar to R_{144} and were not reported for brevity. Acceleration distributions are not reported for brevity.

The values of maximum displacements are higher for options B compared to option A, due to the different distribution of the participating mass in the horizontal modes, especially at mode 4 (cf. Table 4). In particular, for the horizontal responses (R_{144} and R_{441}), $UX/Z_{max} \approx 30/36$ mm and $UY_{max} \approx 7$ mm are obtained for options B, while $UX/Z_{max} \approx 10/11$ mm ($\approx$ -70%) and $UY_{max} \approx 5$ mm ($\approx$ -30%) for option A, and are localised at wrapper foot and inner vessel bottom for all options. A similar trend on the horizontal displacements has been observed for the vertical response (R_{414}).

Quite different pressure distributions can be remarked for horizontal responses: for options B, the maximum hydrodynamic pressure (0.36 MPa) is obtained on the internal side of the inner vessel, while for option A the maximum of 0.48 MPa ($\approx$ +33%) is observed at the plenum-roof interface.

Table 7. Spectrum response, option A.

Comb.	UX (m)	PRES (Pa)
R_{144}	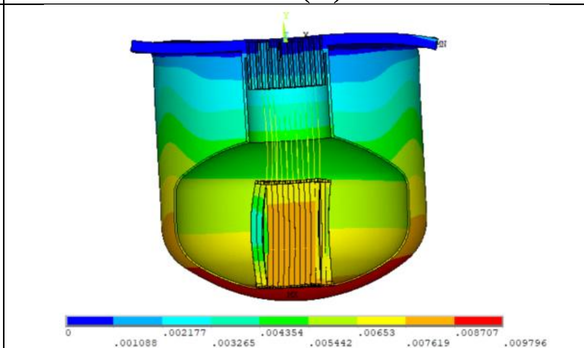	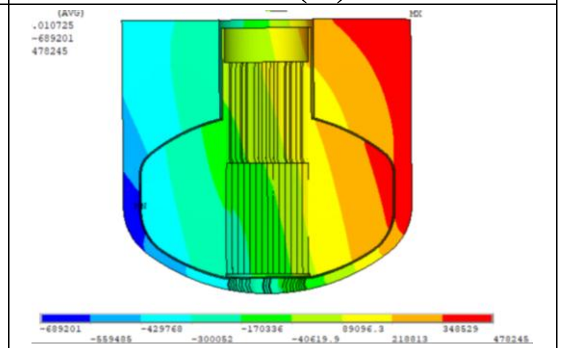
Comb.	UY (m)	PRES (Pa)
R_{414}	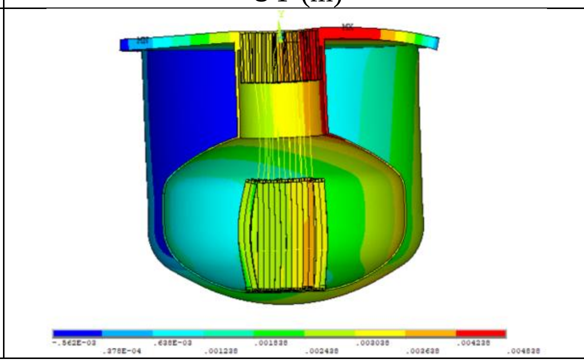	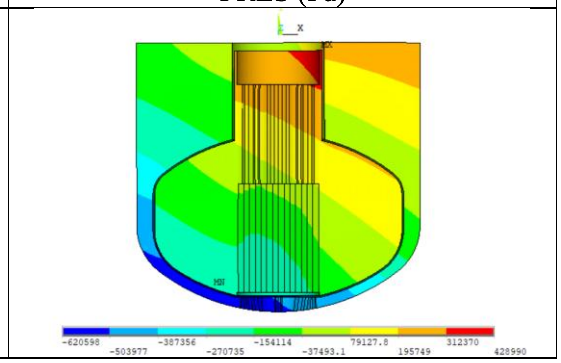

Table 8. Spectrum response, option B.

Comb.	UX (m)	PRES (Pa)
R_{144}	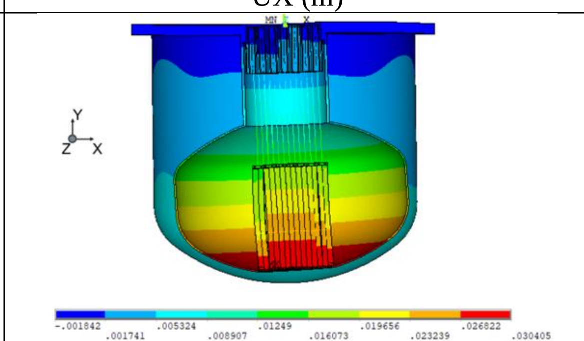	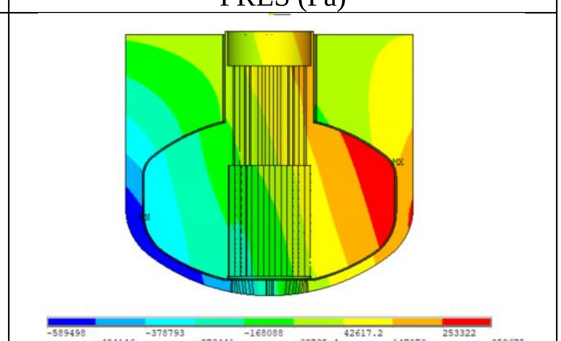
Comb.	UY (m)	PRES (Pa)
R_{414}	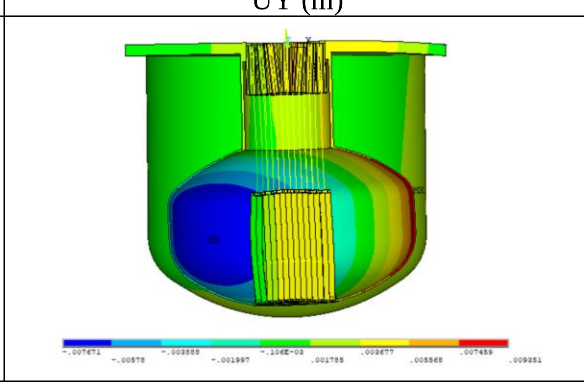	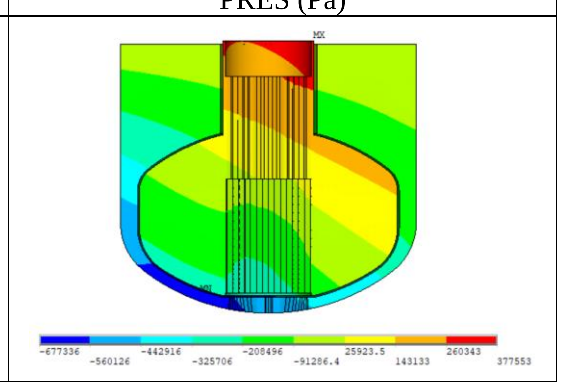

3.2. Buckling analysis of fuel assemblies

Buckling analysis (step 2, cf. Figure 1) was conducted on all FAs. Displacements of the neighbouring fuel assemblies were considered as fixed displacements (computed via the spectrum analysis) at the contact points (see CEX/Y/Z in Figure *1*). Assemblies 1-3 highlighted in Figure 3 were identified as the most critical. This is a pertinent result, since FAs 1-3 are enclosed by the direction of the horizontal seismic responses R_{144} and R_{441}, and they are directly exposed to the lead in the inner vessel (cf. Figure *1*). For brevity, results are reported for FA 1, for which the absolute minimum buckling factor were obtained (slightly higher values were detected for FAs 2 and 3).

A preliminary buckling analysis was conducted by considering only static loads (weight, buoyancy) and thermal expansion effects. The associated results in terms of mode factors (FACT, i.e. collapse load multiplier) and collapse location in the fuel assembly are summarised in Table 9 for static and buckling steps (2a and 2b respectively, cf. Figure 1), together with those of buckling analyses conducted on options A and B. The corresponding displacement distribution are shown in Table 10. Remark that the minimum mode factors were obtained with seismic loads deriving from R_{441}, since response spectrum of direction Z has the maximum acceleration peak (cf. Figure *2*a). Moreover, the maximum displacement of the assembly (U_{max}) resulting from static step (2a, cf. Table 9) are localised at wrapper foot, in agreement with the results of spectrum analysis (cf. Table *7*-Table *8*).

Based on these results, including seismic loading contributions involves an abrupt reduction of mode factors (about one order of magnitude). According to Table 10, structure collapse in options A and B mainly occurs in the wrapper. In particular, it can be remarked that these options show quite similar mode factors and collapse modes, despite A is characterised by a much lower displacement of the wrapper foot. This outcome suggests that the assembly deflection induced by the radial displacement of the inner vessel bottom seems to not significantly impact on the shape of the collapse mode.

It is finally observed that all mode factors obtained for options A and B are higher than the minimum safety factor required by RCC-MRx for service level D (1.35).

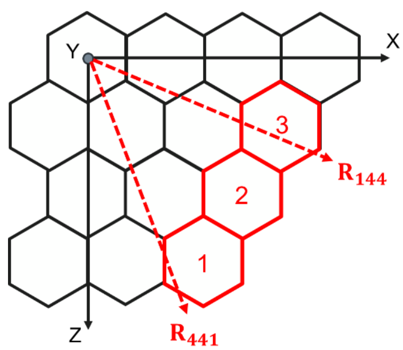

Figure 3. Location of critical fuel assemblies.

Table 9. Buckling analysis, summary of buckling factors and collapse locations.

	Static (2a)		Buckling (2b)					
			Mode 1		Mode 2		Mode 3	
Option–Comb.	U_{max} [mm]	Loc.	FACT	Loc.	FACT	Loc.	FACT	Loc.
Only static loads	0.08	Wrapper centre	89.6	Shaft	182.5	Shaft	293.6	Wrapper
A – R_{441}	8.7	Wrapper foot	1.62	Wrapper	1.78	Wrapper	1.96	Wrapper
B – R_{441}	31.2		1.84	Wrapper	1.94	Wrapper	2.18	Wrapper

Table 10. Buckling analysis, displacement (USUM) distributions.

<table>
<tr><th rowspan="2">Option – Comb.</th><th rowspan="2">Static (2a) USUM (mm)</th><th colspan="3">Buckling (2a) - USUM</th></tr>
<tr><th>Mode 1</th><th>Mode 2</th><th>Mode 3</th></tr>
<tr><td>Only static loads</td>
<td>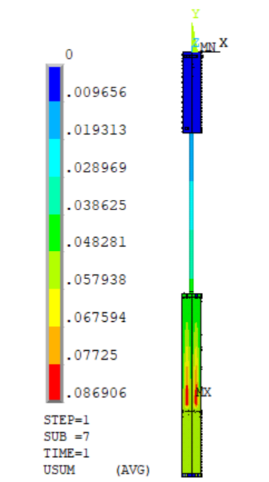
</td>
<td>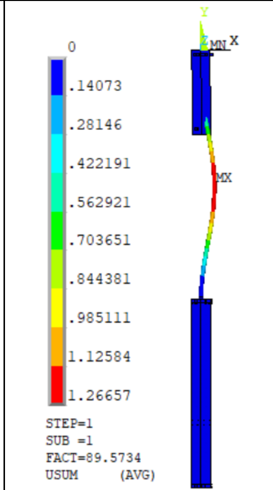
</td>
<td>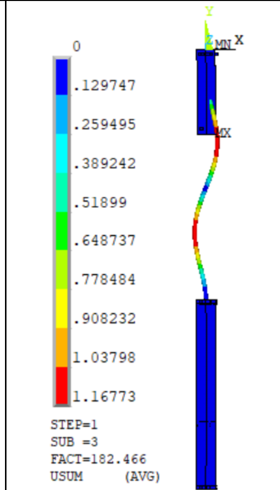
</td>
<td>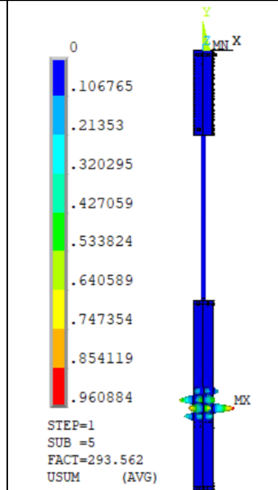
</td></tr>
<tr><td>A – R_{441}</td>
<td>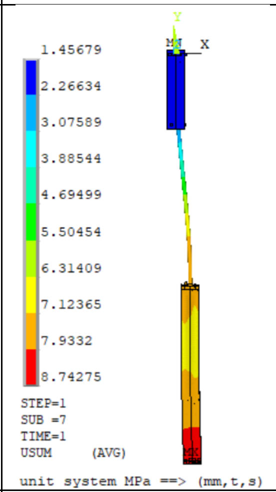
</td>
<td>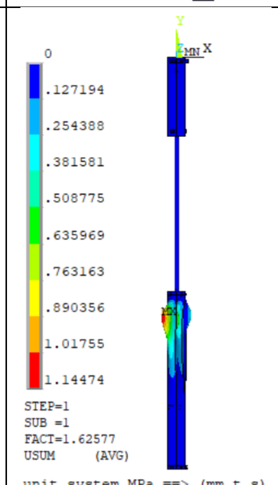
</td>
<td>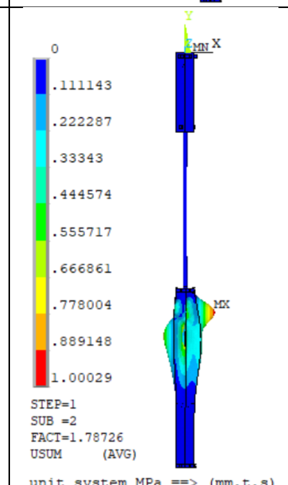
</td>
<td>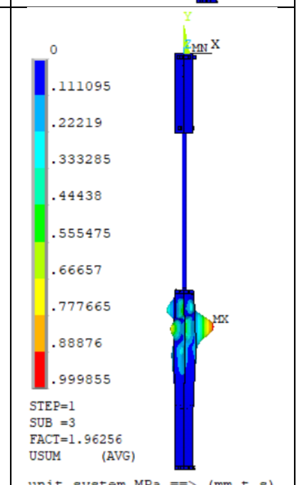
</td></tr>
<tr><td>B – R_{441}</td>
<td>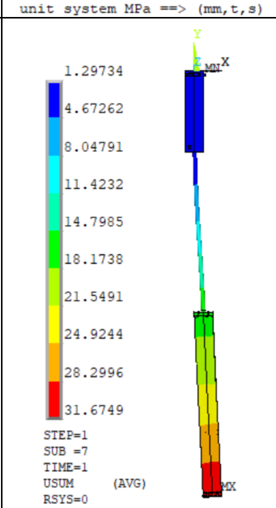
</td>
<td>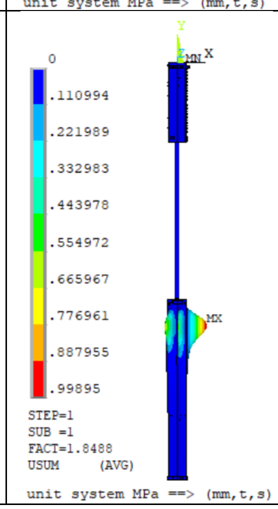
</td>
<td>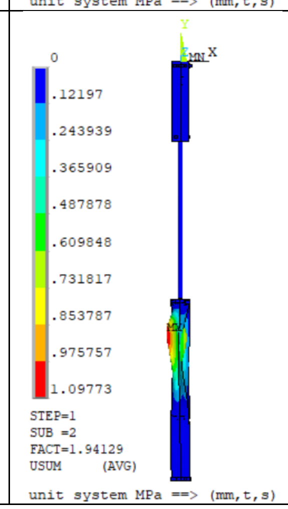
</td>
<td>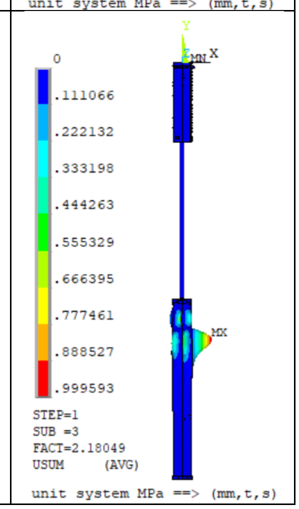
</td></tr>
</table>

4. CONCLUSIONS AND FUTURE WORKS

An application of the acoustic FEM to the seismic analysis of Newcleo's LFR-AS-030 was presented in the current work focusing on the buckling of core structures. A FSI model of the reactor block was implemented in Ansys to compute seismic loading. Calculations were performed with two different modelling options of the reactor plenum (A and B, cf. Figure 2b), in order to investigate the effect of sloshing on the seismic behaviour and on the buckling modes of the fuel assemblies. The presented outcomes must not be intended as the final results of the current configuration of the LFR-AS-30. The final design may be affected by other loads not considered at this stage. Modal and spectrum analyses enabled to identify the main vibration modes of the reactor block considering contact interactions among fuel assemblies and inner vessel, and the associated hydrodynamic pressures and displacements. The subsequent buckling analyses shown that peripheral assembly are more subjected to buckling risk. Collapse mainly occur at wrapper and shaft, which are the slenderest parts of the fuel assembly. Concerning the most critical buckling modes, the displacement of the fuel assembly lower part (wrapper foot) seems not to have a significant impact on buckling factors, while allowing free surface sloshing in the plenum (option B) involves slightly lower load multipliers.

Newcleo's research program includes future benchmarks via CFD calculations to improve the modelling of sloshing and of non-linear FSI effects, and experimental campaigns for validating the results. Calculation activities for elastic-plastic buckling analysis of fuel assembly structures are also foreseen.

REFERENCES

Newcleo official site, *www.newcleo.com/products-services/delivering-our-gen-iv-vision*.

EN 1998-4, Eurocode 8 – *Design of structures for earthquake resistance – Part 4: Silos, tanks and pipelines*, 2006.

American Society of Civil Engineers (ASCE), *Seismic Analysis of Safety-Related Nuclear Structures and Commentary*, 2016.

New Zealand Society for Earthquake Engineering (NZSEE), *Seismic Design of Storage Tanks*, 2009.

C. Yu, A. S. Whittaker, "Analytical Solutions for Seismic Fluid-Structure Interaction of Head-Supported Cylindrical Tanks", *Journal of Engineering Mechanics*, vol. 146, 2020.

C. Yu, A. S. Whittaker, "Analytical and Numerical Studies of Seismic Fluid-Structure Interaction in Liquid-Filled Vessels", *Earthquake Engineering to Extreme Events*, MCEER-20-0003 (2021).

M.Z.Kangda, S.S.Sawant, O.R.Jaiswa, "Sloshing in liquid storage tanks with internal obstructions", *Structural Engineering Convention* (SEC-2016).

J.-F. Sigrist, "Modal analysis of fluid-structure interaction problems with pressure-based fluid finite elements for industrial applications", *International Journal of Multiphysics*, vol. 1, no. 1, pp. 123-151, 2007.

M. Platti, "Seismic sloshing in a suspended structure with internals", *POLITesi - Archivio digitale delle tesi di laurea e di dottorato* (2015-2016).

Sang Yun Je, Yoon-Suk Chang, Sung-Sik Kang, "Dynamic characteristics of reactor vessel internals with fluid-structure interaction", *Nuclear Engineering and Technology* 49 (2017) 1513-1523.

Afcen RCC-MRx, *Design and construction rules for mechanical components of nuclear installations: high temperature, research and fusion reactors*, Section III – Tome I (2018).

D. Panico, D. Tomatis, "lbh15: a Python package lead, bismuth, and lead-bismuth eutectic thermophysical properties for fast reactor applications", *Proceedings of 20th International Topical Meeting on Nuclear Reactor Thermal Hydraulics* (NURETH-20), Washington DC, USA, pp. 1-12, 2023.

U.S. Nuclear Regulatory Commission (2012), *Regulatory Guide 1.92 – Combining modal responses and spatial components in seismic response analysis*, revision 3.